

Polarized Neutron Reflectometry on Exchange Coupled Superlattices

Andreas Schreyer

Experimentalphysik (Festkörperphysik), Ruhr-Universität Bochum, D-44780 Bochum, Germany

(Received 27 January 1996; accepted 14 June 1996)

Following a brief introduction to the theory of polarized neutron reflectometry with polarization analysis, applications of the technique to exchange coupled superlattices with various different magnetic structures are presented. First, the sensitivity of the method to the orientation of the in-plane magnetic moment is demonstrated quantitatively by studying the effect of sample reorientation. Then results on the oscillatory exchange coupling in Co/Cu(111) superlattices are discussed. Finally, we show how the coupling angle in non-collinearly coupled Fe/Cr(001) superlattices can be determined quantitatively.

KEYWORDS: magnetic superlattices, neutron reflectometry, polarization analysis, oscillatory exchange coupling, non-collinear coupling

§1. Introduction

The recent increase in popularity of neutron reflectometry (NR) has been driven by a massive growth of interest in the properties of layered thin film structures which growers have learned to prepare with unprecedented quality during the 1980's. For the study of magnetic thin film systems polarized beam techniques were quickly added.¹⁾ In this paper we want to discuss recent polarized neutron reflectometry (PNR) results on exchange coupled magnetic multilayer systems of various magnetic structures in ascending order of complexity. Special emphasis will be given to PNR with polarization analysis since it provides the most detailed insights into the magnetic structures. At the same time this paper will give an overview of magnetic coupling phenomena which can be encountered in magnetic thin film systems.

§2. Theory

In (specular) reflectometry we consider the condition that the angles Θ of incidence and reflection of neutrons of wavelength λ with respect to the sample surface are equal, i.e., the scattering vector $|\mathbf{Q}| = 4\pi/\lambda \cdot \sin \Theta$ is perpendicular to the sample surface. The process of reflection of polarized neutrons is described by the coupled system of Schrödinger equations

$$\frac{\partial^2}{\partial z^2} \Psi_{\pm}(z) + \left[\frac{Q^4}{4} - \frac{2m_n}{\hbar^2} V_{\pm\pm}(z) \right] \Psi_{\pm}(z) - \frac{2m_n}{\hbar^2} V_{\pm\mp}(z) \Psi_{\mp}(z) = 0 \quad (1a)$$

$$\frac{\partial^2}{\partial z^2} \Psi_{\mp}(z) + \left[\frac{Q^4}{4} - \frac{2m_n}{\hbar^2} V_{\mp\mp}(z) \right] \Psi_{\mp}(z) - \frac{2m_n}{\hbar^2} V_{\mp\pm}(z) \Psi_{\pm}(z) = 0 \quad (1b)$$

where the z axis is perpendicular to the sample surface (i.e., $\parallel \mathbf{Q}$), m_n is the neutron's mass, $\pm(-)$ denotes the up (down) spin state of the neutrons in a magnetic field, and the scattering potentials V_{ij} are

$$\begin{pmatrix} V_{++} & V_{+-} \\ V_{-+} & V_{--} \end{pmatrix} = \frac{2\pi\hbar^2}{m_n} n_0 \left[\begin{pmatrix} b^n & 0 \\ 0 & b^n \end{pmatrix} \begin{pmatrix} P_y & P_x \\ P_x & -P_y \end{pmatrix} \right] \quad (2)$$

for the case of an external magnetic field in the sample plane, i.e., $\perp z$. Here n_0 is the atomic number density, b^n is the coherent nuclear scattering length, p is the magnetic scattering length, and $\mathbf{p} = p\mathbf{m}$ is a magnetic scattering length vector resulting from magnetic moments μ in one magnetic domain which are parallel to the unit vector \mathbf{m} in the sample plane with the geometry shown in Fig. 1. From Eq.(2) it follows that, apart from a constant factor, the scattering potential V_{ij} corresponds to a scattering length density $n_0 b^{\text{eff}} = n_0(b^n + p_\kappa)$.

The following conclusions can be drawn. When the V_{ij} with $i \neq j$ are zero, Eqs. (1a) and (1b) are decoupled and no *spin flip* (SF) occurs, i.e., the neutrons maintain their spin state upon interaction with the sample. This case is called *non-spin-flip* (NSF) scattering. From Eq. (2) and Fig.1 it follows that any non-vanishing \mathbf{p} would have to be oriented along the y -axis. Alternatively, any x -component of \mathbf{p} would induce SF scattering. Thus, by distinguishing between NSF and SF scattering, quantitative analysis of PNR data yields the *orientation of any magnetic moments in the sample plane*. In Fig.1

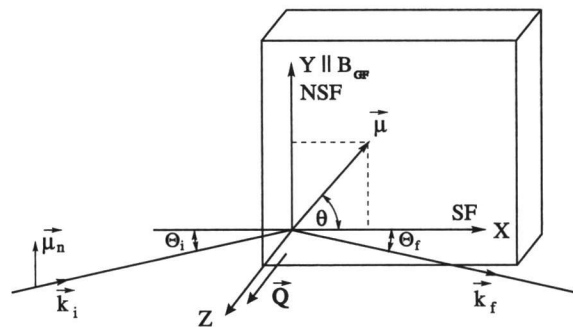


Fig. 1. Schematic of the scattering geometry. The scattering triangle with the incident and final wavevectors \mathbf{k}_i and \mathbf{k}_f is shown with the scattering vector \mathbf{Q} parallel to z . A small external neutron guide field B_{GF} is oriented along y to provide a polarization axis of the neutron magnetic moments μ_n parallel to y . NSF scattering occurs for y - and SF scattering for x -components of any magnetic moments μ in a single domain in the sample plane.

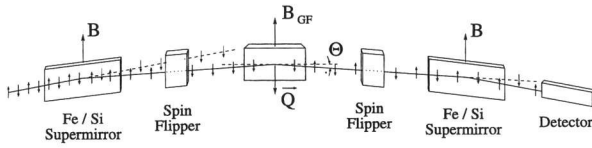


Fig. 2. Schematic of the reflectometer BT-7 showing the elements behind the monochromator. The instrument is shown reflecting the (-) cross section with both spin flippers on. The small arrows denote the spin state of individual neutrons. The polarizing supermirrors only reflect the (+) spin state.

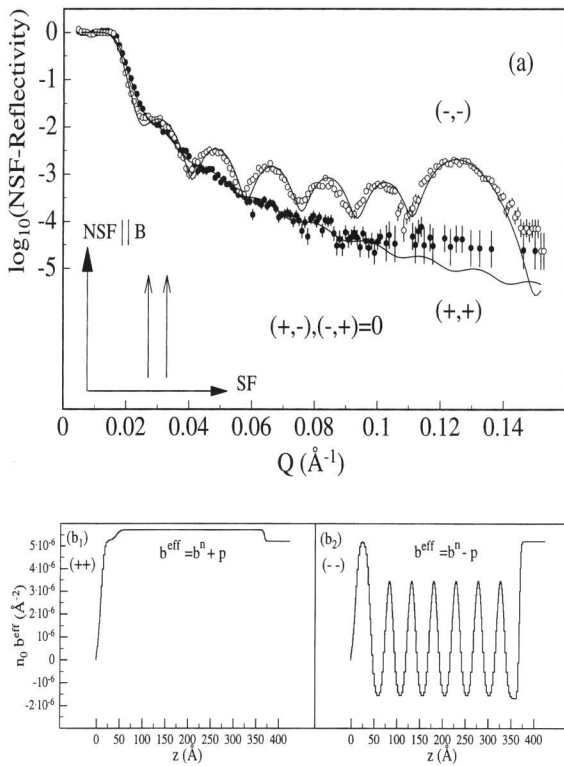


Fig. 3. (a) PNR of a Co/Cu multilayer with ferromagnetically ordered Co moments oriented along the NSF axis with fits to the data. The moment orientations are indicated in the inset. No SF reflectivity was detected in (a). (b) Scattering length density profiles from which the lines in (a) were calculated; (b_1) corresponds to the (+) and (b_2) to the (-) cross section. The sample surface is at $z=0$.

the scattering geometry is summarized. The y and x axes are denoted as the NSF and SF axes, referring to the kind of scattering the respective component of p causes. Solutions of Eq.(1) have been provided by various authors.¹⁻⁵⁾ To analyze data, theoretical reflectivities are calculated assuming a potential wall structure $V_{ij}(z)$ made up of slabs of constant potential with sharp interfaces in between. Interface roughness, as it occurs in realistic samples, can best be included via a large number of infinitely thin slabs of gradually varying potential.⁶⁾ Then $V_{ij}(z)$ is varied to fit the calculated reflectivities to the measured data.⁶⁻⁸⁾

§3. Experimental

The data discussed in this paper were taken on the reflectometer BT-7³⁾ at the Research Reactor of the National Institute of Standards and Technology in Gaithersburg, USA. In Fig.2 a schematic of the instrument is shown. A monochromatic beam ($\lambda = 2.367 \text{ \AA}$) is polarized, passing through a spin flipper⁹⁾, reflected by the sample, passing through another spin flipper, polarization-analyzed, and then detected. Q is varied in standard $\Theta/2\Theta$ mode. Collimation slits (not shown in Fig.2) provide a horizontal angular beam divergence $\Delta\Theta \approx 0.3 \text{ mrad}$. Polarization analysis is essential to distinguish between NSF and SF scattering, which in turn provides the sensitivity to the orientation of magnetic in-plane moments, as discussed above. By setting both spin flippers to 'off' or 'on', the (++) and (--) cross sections can be distinguished. The latter case is depicted in Fig.2. On the other hand, the combination of flippers 'on'-'off' and 'off'-'on' yields the (+-) and (-+) cross sections, respectively.

The following corrections were applied to the data.⁸⁾ To obtain the true specular reflectivity, a diffuse (off-specular) background reflectivity measured in $[(\Theta - \delta\Theta)/2\Theta]$ mode, i.e., with a small offset $\delta\Theta = 0.1$ to 0.2° in Θ , was subtracted. To account for the never-perfect efficiency of the polarizing elements an elaborate correction formalism⁴⁾ was used, yielding efficiencies in the 95-99% range for all polarizing elements. A final simple correction accounts for the increase in the measured intensity which is induced by the change of the sample cross section with respect to the incoming beam with growing Θ .

§4. Results

§4.1 Tutorial

An instructive example for the sensitivity of PNR with polarization analysis to the moment orientation is provided in Fig.3.⁸⁾ The data were taken using a $[\text{Cu}_{15}/\text{Co}_{34}]^7)$ multilayer which had been sputtered onto a $\text{Al}_2\text{O}_3(11\bar{2}0)$ substrate using techniques described elsewhere.¹⁰⁾ As for the rest of this paper the subscripts denote the individual layer thicknesses in \AA , whereas the superscript N_Λ gives the number of bilayers. A strong uniaxial in-plane anisotropy aligns all Co moments along one easy axis, thus providing a comparatively simple magnetic structure. By simply rotating the sample, the orientation dependence of PNR described in §.2 can now be checked quantitatively. In Fig.3 (a) the Co moments were oriented along the NSF axis as indicated by the inset. Consistent with the discussion of §.2, no SF scattering was detected due to the absence of any moment component along the SF axis. On the other hand, the NSF scattering is strongly split as a consequence of the large diagonal terms in Eq.(2). The splitting is a measure of the magnitude of the magnetic moment. In Fig.3(b) the effective scattering length density profiles $n_0 b^{\text{eff}}$ are shown, from which the fitted lines in Fig.3(a) were calculated. Fig.3(b) is the potential wall structure mentioned in §.2. Close inspection shows how the

structure was constructed from thin slabs to model a periodic multilayer with rough interfaces.

To fit the data, a non-magnetic oxide had to be assumed near the sample surface at $z=0$. In the $40 \text{ \AA} \leq z \leq 370 \text{ \AA}$ region the periodic structure of the subsequent Co/Cu layers can be seen for $b^{\text{eff}} = b^n - p$ in Fig.3(b₂). At largest z the layer sequence terminates with the substrate. The profile in Fig.3(b₂) causes the (--) cross section in Fig.3(a), leading to pronounced oscillations. The peak around $Q_{\text{ML}} \approx 0.125 \text{ \AA}^{-1}$ is due to the period Λ of the multilayer which is the sum of the individual Co and Cu thicknesses. The fitted value of Λ is found to coincide with the nominal one (49 \AA) within a few percent. The oscillations of period $2\pi/D$ between the superlattice peak and the critical Q of total external reflection $Q_C \approx 0.015 \text{ \AA}^{-1}$ are the $N_{\Lambda} - 2$ Kiessig fringes which are a measure of the total thickness D of the film on the substrate. They originate from the interference of beams reflected from the sample surface and the substrate. The multilayer peak is shifted due to the total external reflection regime:

$$Q_{\text{ML}}^n = \sqrt{Q_C^2 + \left(n \cdot \frac{2\pi}{\Lambda}\right)^2} \quad (3)$$

For $b^{\text{eff}}=b^n+p$ (Fig.3(b₁)) no contrast exists between the Co and Cu layers. Also the contrast between the Co/Cu region and the substrate is small, explaining the lack of structure in the (++) data in Fig.3(a).

The drastic effect of sample reorientation is visible in Fig. 4.⁸⁾ The sample has been turned clockwise by 90° , aligning the Co moments with the SF axis. Consequently, strong SF scattering is observed whereas the splitting of the NSF reflectivities vanishes completely, fully consistent with Eq.(2). The superlattice peak and the Kiessig fringes are now observed in all cross sections. The scattering length density profiles, which differ from the ones discussed previously only by setting θ to zero (see Fig. 1. and Eq. (2)), show a purely nuclear profile for NSF (Fig.4(b₁)) and a purely magnetic profile for SF scattering (Fig. 4 (b₂)). An interesting effect can be observed in the total reflectivity region below Q_C . The NSF reflectivity is strongly reduced in the region of maximum SF reflectivity. This is a result of the fact that the conditions of total reflection now are $R(++)+R(+)=1$ and $R(--)+R(-)=1$, since the possibility of a spin flip has to be included for each of the spin states (+) and (-) of the incident beam.¹¹⁾

To model the data a reduction of n_0 of Co and Cu and a significant intermixing of both materials had to be assumed.⁸⁾ This can be seen most drastically in Fig. 4 (b₂) where the purely magnetic scattering length density $n_0 p$ does not go to zero even in the Cu layers. However, due to their strong uniaxial anisotropy these samples were ideally suited to quantitatively compare the theoretically expected orientation dependence of the in-plane magnetization on the PNR with experiment. Actually, this uniaxial anisotropy turned out to be very interesting by itself. It seems to be due to a partial internal oxidation of Co atoms at the Co/Al₂O₃ interface by the topmost oxygen atoms of the Al₂O₃, which appear to be

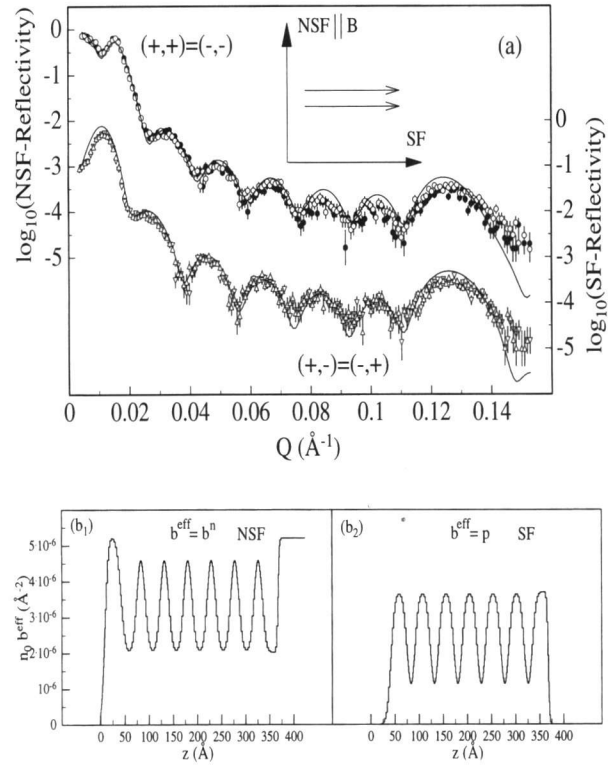


Fig. 4. (a) PNR of a Co/Cu multilayer with ferromagnetically ordered Co moments oriented along the SF axis with fits to the data. The SF data have been offset by 10^{-2} and are plotted against the scale on the right hand axis. The moment orientations are indicated in the inset. (b) Scattering length density profiles from which the lines in (a) were calculated; (b₁) corresponds to the NSF and (b₂) to the SF cross sections.

lined up with the hard axis of the anisotropy in the Co.^{11,12)} Furthermore, the strong uniaxial anisotropy favours a magnetic one-domain state even in remanence. This property considerably simplifies the data analysis. More complicated cases will be discussed below.

§4.2. Oscillatory exchange coupling

One of the most intriguing discoveries in the research on thin magnetic films was that of an oscillatory exchange coupling between FM layers over non-FM layers. It was found that period, phase, and intensity of the oscillations sensitively depend on the material in the non-FM interlayer, its thickness, and on the growth direction.¹³⁾ The system Co/Cu was an important model system, since it can be grown epitaxially in the [001], [110], and [111] directions in a coherent *fcc* structure. Furthermore, strong oscillatory coupling was predicted theoretically for all growth directions.¹⁴⁾ However, whereas the coupling was easily found for the [001]¹⁵⁾ and [110]¹⁶⁾ growth directions, the initial results were very discouraging for epitaxially grown, well ordered [111] samples.

As is well known, neutron methods are ideally suited to provide direct proof of AF structures. In PNR the doubling of the magnetic period over the chemical one is reflected by additional superlattice peaks of purely magnetic origin, occurring roughly at positions half way between the Q_{ML}^n and between Q_C and Q_{ML}^1 .

In Fig. 5 the PNR data are presented, which finally

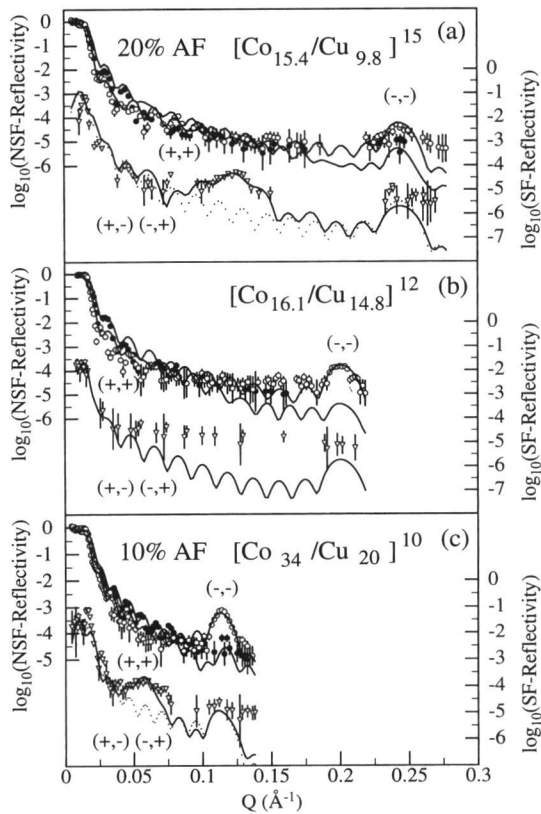


Fig.5. PNR of three Co/Cu(111) superlattices with the structure indicated in each of the figures together with model fits (solid and dotted lines) as discussed in the text. The dotted lines in (a) and (c) were calculated assuming a purely FM structure. The data were taken in a small neutron guide field of 14 G. Again the SF data have been offset by 10^{-2} and are plotted against the scale on the right hand axis.

confirmed the existence of an oscillatory exchange coupling also in Co/Cu(111).¹⁷⁾ Shown in Fig.5 are the PNR of three Co/Cu(111) superlattices of increasing Cu interlayer thicknesses. Before starting the scans each sample had been magnetized in a few hundreds Gauss along the NSF axis. Since, as expected, the SF cross sections were equal in this experiment, they were added to improve counting statistics. In some regions of the data no specular intensity is observed due to the background subtraction. The data points adjacent to these regions should therefore be taken as upper limits for the actual intensity in these regions, which was too low to be detectable. All NSF (--) data sets show a regime of total external reflection up to Q_C^{NSF} at low Q , Kiessig fringes, and the first superlattice peak around the highest Q at $Q = Q_{ML}^1$. The NSF(++) and SF data, on the other hand, exhibit weak or no superlattice peaks at Q_{ML}^1 . This feature can only be explained as a consequence of at least a major part of the Co moments being aligned parallel to the initially applied field along the NSF-axis. This leads to the lack of contrast between Co and Cu for the NSF(++) cross sections and to the splitting of the NSF cross

sections, which is typical for ferromagnetically coupled Co/Cu superlattices with the Co moments aligned along the NSF axis (see discussion of Fig.3 above). Consequently, at least a major part of the sample area must be FM in all samples. Whereas in Fig.5(b) no peak in the SF scattering is observed, the scans shown in Figs.5(a) and (c) both clearly exhibit a peak at the respective half-order nuclear peak position. Therefore these data unambiguously prove that the samples with $t_{Cu}=9.8$ Å and with $t_{Cu}=20$ Å contain coherent spin structures, which are consistent with an AF coupling between the Co layers. Since the SF cross sections contain information solely on the components of the Co moments which are parallel to the SF-axis, the AF coupled regions have been forced into the spin flop state by the initially applied field. The fact that the sample with $t_{Cu}=16.1$ Å (Fig.5(b)) does not exhibit a half-order peak confirms the spacer thickness dependence expected for an oscillatory exchange coupling.

In the following we will discuss the modeling of the data in more detail than in our initial publications.^{17,18)} The theoretical reflectivities in Fig.5 were calculated assuming the presence of a majority FM coupled component in the samples. To reproduce the observed intensities a significant intermixing of the Co and Cu layers had to be assumed for all three samples, consistent with x-ray data. The intermixing reduced the (--) scattering contrast between Co and Cu, leading to a significant reduction of the respective first superlattice peak intensities to the observed values. The most important result is that a reduction of the scattering length density of the Cu spacer layers by up to 25% was found together with a corresponding non zero magnetic moment due to the presence of Co in the supposedly non-magnetic spacer. In a scanning tunnel microscope (STM) study it was demonstrated at the same time that the observed large intermixing is a result of the growth of Co islands on Cu(111) instead of a smooth film.¹⁹⁾

Since the sample has FM and AF coupled regions, the question arises how the scattering from these regions has to be superimposed in the calculations. In principle there are two ways. In the first case it is assumed that both regions scatter *incoherently*, i.e., no coherent interaction between the reflected amplitudes \mathfrak{R}_{ik}^j from regions $j=1,2,3,..$ occurs. Then, the average of the reflected intensities

$$R_{ik} = |\mathfrak{R}_{ik}|^2 = \sum_j c_j |\mathfrak{R}_{ik}^j|^2 \quad (4)$$

is taken, where the c_j denote the relative contribution from region j with $\sum_j c_j = 1$. In the other case *coherent* interaction of the amplitudes \mathfrak{R}_{ik}^j is assumed, i.e., the averaging is performed before squaring the amplitudes:

$$R_{ik} = |\mathfrak{R}_{ik}|^2 = \left| \sum_j c_j \mathfrak{R}_{ik}^j \right|^2 \quad (5)$$

An important consequence is, that in the latter case the presence of domains with various orientations can lead to a reduced average magnetic scattering length density and thus to a reduced Q_C^{NSF} compared to a pure one-domain case.

Due to the measured Q_C^{NSF} , the data of Fig.5(a) and (c) can be better fitted by coherent superposition and by

assuming that only 48% (a) (67.5% (c)) of the magnetic moment is aligned along the NSF axis. Only 20% (a) (10%(c)) of the moments are found to be coupled AF and oriented along the SF axis, causing the broad half-order peaks. The remaining 32% (a) (22.5% (c)) of the moment are oriented along the SF axis and are FM coupled. For the purely FM data of Fig.5(b) 80% of the moment was assumed to be parallel and 20% perpendicular to the NSF axis. The incomplete alignment of the sample's FM components, despite the initial magnetization along the NSF axis, is not unexpected since FM systems are well known to have a lower magnetization in the remanent state than in the saturated state, due to energetically favorable domain formation. Whereas the fitting results regarding the significance of the FM SF component may be somewhat ambiguous due to the large error bars and missing data points resulting from the background subtraction, the results for the magnitude of the AF components are not affected by these uncertainties. To account for the observed broadness of the half-order peaks in Fig.5(a) and (c), a reduction of the coherence lengths of the AF coupled regions to 40% of the nuclear coherence length (=total thickness) had to be assumed. Therefore, only 6 (4) of the Co layers were found to be coupled AF for the cases of Fig.5(a) and (c), respectively.

Nevertheless, the dotted lines in both figures, which were calculated for a purely FM structure, clearly confirm that an AF component has to be included to explain the data, proving the oscillatory nature of the coupling. These results agree well with MOKE hysteresis measurements yielding an oscillation period of 9 Å, consistent with theory and an AF component of the same magnitude as detected by PNR.¹⁷⁾ It should be stated, however, that MOKE can not provide direct proof of AF structures.

§4.3. Non-collinear coupling

In 1991 strong evidence was found that apart from collinear FM and AF, non-collinear magnetic structures can also exist in transition metal superlattices.^{20,21)} Due to its sensitivity to the in-plane moment orientation, PNR with polarization analysis is ideally suited to study such structures. In Fig.6 PNR data from a non-collinearly coupled Fe/Cr(001) superlattice are shown^{22,23)}. Again the sample was magnetized along the NSF axis in 7.3 kG before the experiment. Clearly, the NSF reflectivities are split and additional strong SF scattering is observed. All reflectivities exhibit first-order superlattice peaks at $Q_{ML}^1 \approx 0.09 \text{ \AA}^{-1}$. In addition, half-order peaks at about $Q_{ML}^1/2$ are observed in all reflectivities. These result from a doubling of the magnetic periodicity over the nuclear one, as would be seen in a collinear AF structure. Such an AF structure would have no resulting moment. However, the splitting of the NSF data and the existence of a first-order peak in the SF data clearly indicate that a finite moment is projected along the NSF and SF axes in every layer. Therefore, the half-order peaks can only be caused by a non-collinear moment orientation. The simplest assumption would be a perpendicular orientation of the

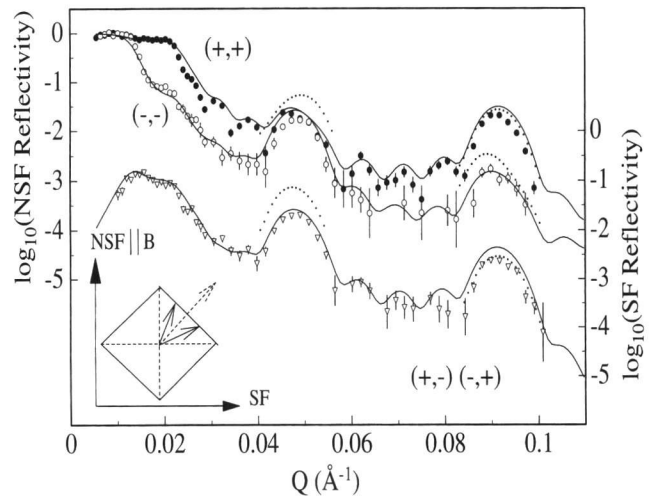


Fig.6. PNR of a $[\text{Fe}_{52}/\text{Cr}_{17}]^9$ superlattice grown at 250°C taken in a small neutron guide field of 17 G together with model calculations for a coupling angle of 90° (dotted lines) and 50° (solid lines). The latter case is depicted in the inset which shows a top view of the sample with its in-plane easy axes of the magnetocrystalline anisotropy (dashed lines). Again the SF data have been offset by 10^{-2} and are plotted against the scale on the right hand axis.

moments along the two easy axes (dashed lines in the inset). Nevertheless, the calculated SF and NSF reflectivities for this magnetic structure (small dots in Fig.6) show that the data are not consistent with such a 90° model. On the other hand, if non-perpendicular orientation is allowed, the data can be well fitted (solid line in Fig.6) by assuming a coupling angle of $\phi_c = 50^\circ \pm 4^\circ$ between the adjacent Fe layers, as schematically depicted by the solid arrows in the inset of Fig.6. Input to the model calculation was the sample structure as determined from the x-ray fits and the Fe magnetic moment as found by PNR in the saturated state. The only fit parameters left are the orientations of the moments in the Fe layer.

By performing measurements as in Fig.6 as a function of external magnetic field, we were able to obtain new detailed information about the exchange coupling energy in the Fe/Cr system.^{22,23)} Such data contains much more information than any other magnetometry method since these only yield a resultant magnetization.

As detailed elsewhere²³⁾ domains only complicated the modeling very close to remanence. At slightly higher fields the sample was in a single domain state. However, even in the multi-domain state detailed analysis shows that only two domain types contribute to the scattering. Furthermore, incoherent averaging (Eq.(4)) had to be assumed in this case. Using Eq.(5) or assuming other domain types would have led to massive contradictions with the measured field dependent PNR data.²³⁾ Comparing the contradictory results for Co/Cu(111) and Fe/Cr(001) on the averaging process, two facts can be stated. First, the coherence length of the incident neutrons l_c^{\parallel} parallel to the sample surface as calculated from first principles²⁴⁾ can not be the relevant parameter

since in both cases it is of the order of the sample size (cm). Second, following STM results¹⁹⁾ in the case of Co/Cu(111) the lateral dimension of the AF and FM coupled regions will be of order 100 Å whereas for Fe/Cr(001) the magnetic domains were found to be about 20 μm in diameter by Kerr microscopy. Thus we may conjecture that the averaging process is determined by the lateral length scale of the magnetic domains whereas l_c^{\parallel} only provides an upper limit of coherent averaging.

Finally it should be pointed out that the data of Fig.6 can not be explained by assuming a coexistence of AF and FM domains as in the case of Co/Cu(111). The initial magnetization of the sample in 7.3 kG would have induced FM domains predominantly oriented along the NSF axis and AF domains oriented in a spin flop state along the SF axis, i.e., along both easy axes of the anisotropy. However, this structure neither accounts for the strong half order NSF peak nor for the strong first order SF peak in the data. Model calculations which take into account the role of the magnetocrystalline in-plane anisotropy^{22,23)} confirm that the moments align as closely with the easy axes as allowed for by the non -90° coupling angle, leading to the structure depicted in the inset of Fig. 6. Thus, the additional peaks in Fig. 6 are a direct consequence of non-collinear coupling. On the other hand, however, we can not exclude a non-collinear magnetic structure in the Co/Cu(111) system. Due to the absence of a comparable in-plane anisotropy, the initial magnetization process could also lead to the observed spectra in Fig. 5 (a) and (c) in the case of a non-collinear structure. For the observation of the oscillatory nature of the coupling, however, this point is of minor importance.

§5. Conclusions

We have demonstrated quantitative agreement between theory and experiment concerning the orientation dependence of the in-plane magnetic moment for the example of the reorientation of an FM multilayer. Furthermore we have discussed in detail how by using polarization analysis AF and FM components of different orientations can be distinguished in Co/Cu(111) superlattices which were shown to exhibit oscillatory exchange coupling. Finally we demonstrated the application of PNR with polarization analysis for the determination of non-collinear magnetic structures. It can be stated that PNR with polarization analysis can provide information on the magnetic structure of thin film systems which can hardly be obtained otherwise. Currently we are building the new CRG-B instrument ADAM at the ILL in Grenoble / France which is specifically designed for such experiments.²⁵⁾

Acknowledgements

I gratefully acknowledge the fruitful collaboration with J.F. Ankner and C.F. Majkrzak at NIST who have contributed much more than just beamtime to this work. Furthermore I thank P. Bödeker, Ch. Morawe, K. Theis-Bröhl, M. Schäfer, and P. Grünberg for the samples and H. Zabel for many discussions of the topic. Financial support was provided by NATO (CRG901064) and the German BMBF (ZA3BOC) and DFG via SFB 166.

- 1: G.P. Felcher et al.: *Rev. Sci. Instrum.* **58** (1987) 609.
- 2: C.F. Majkrzak: *Physica B* **156 & 157** (1989) 619.
- 3: C.F. Majkrzak: *Physica B* **173** (1991) 75.
- 4: C.F. Majkrzak: *Physica B* (1996), (in print.ing)
- 5: S.J. Blundell and J.A.C. Bland: *Phys. Rev. B* **46** (1992) 3391.
- 6: J.F. Ankner: in "Surface X-Ray and Neutron Scattering", edited by H. Zabel and I.K. Robinson, Springer Proceedings in Physics (Springer, Berlin, 1992), **61**, p. 105.
- 7: J.F. Ankner: (to be published).
- 8: A. Schreyer: *Ph. D. Thesis, Ruhr-Universität Bochum* (1994), in English, available via the WWW at <http://www.ep4.ruhr-uni-bochum.de/people/as>.
- 9: C.F. Majkrzak and G. Shirane: *Jour. de Phys. (Paris)* **43** (1982) C7-215.
- 10: Ch. Morawe et al.: *J. Magn. Magn. Mater.* **102** (1991) 223, *J. Mater. Res.* **9** (1994) 570.
- 11: A. Schreyer et al.: *J. Appl. Phys.* **73** (1993) 7616.
- 12: N. Metoki et al.: *J. Magn. Magn. Mater.* **118** (1993) 57.
- 13: see e.g. the review of B. Heinrich and J.F. Cochran: *Adv. Phys.* **42** (1993) 523.
- 14: P. Bruno and C. Chappert: *Phys. Rev. Lett.* **67** (1991) 1602, *Phys. Rev. B* **46** (1992) 261.
- 15: M.T. Johnson et al.: *Phys. Rev. Lett.* **68** (1992) 2688.
- 16: M.T. Johnson et al.: *Phys. Rev. Lett.* **69** (1992) 969.
- 17: A. Schreyer et al.: *Phys. Rev. B* **47** (Rapid Communications) (1993) 15334.
- 18: J.F. Ankner et al.: in "Magnetic Ultrathin Films, Multilayers, and Surfaces", edited by C. Chappert et al., MRS Symposia Proceedings, (Materials Research Society, Pittsburgh, 1993) **313**, p. 213.
- 19: J. de la Figuera et al.: *Phys. Rev. B* **47** (1993) 13043.
- 20: M. Rührig et al.: *Phys. Stat. Sol. (a)* **125** (1991) 635.
- 21: B. Heinrich et al.: *Phys. Rev. B* **44** (1991) 9348.
- 22: A. Schreyer et al.: *Europhys. Lett.* **32** (1995) 595.
- 23: A. Schreyer et al.: *Phys. Rev. B* **52** (1995) 16066.
- 24: H. Rauch: in "Neutron Interferometry", edited by U. Bonse and H. Rauch (Clarendon Press, Oxford, 1979), p. 174.
- 25 for details see <http://www.ep4.ruhr-uni-bochum.de/>